Cell Communication and Signaling

RESEARCH

Open Access

Gamma-glutamyl transferase secreted by *Helicobacter pylori* promotes the development of gastric cancer by affecting the energy metabolism and histone methylation status of gastric epithelial cells

Xin Jiang[1†], Weijun Wang[1†], Zeyu Wang[1], Zhe Wang[1], Huiying Shi[1], Lingjun Meng[1], Suya Pang[1], Mengke Fan[1] and Rong Lin[1*]

Abstract

Background *Helicobacter pylori* (*H. pylori*) infection is critical in the development and occurrence of gastric cancer. *H. pylori* secretes gamma-glutamyl transferase (GGT), which affects energy metabolism and histone methylation in mesenchymal stem cells. However, its effect on human gastric epithelial cells remains unclear. This study aimed to investigate the effects of GGT on energy metabolism and histone methylation in gastric epithelial cells and determine its role in the development and progression of *H. pylori*-induced gastric cancer.

Methods A *GGT* knockout *H. pylori* strain and mouse gastric cancer model were constructed, and alpha-ketoglutarate (α-KG) was added. The underlying mechanism was investigated using proteomics, immunohistochemistry, Western blotting, and other experimental assays.

Results *H. pylori* can colonize the host's stomach and destroy the gastric epithelium. GGT secreted by *H. pylori* decreased the concentration of glutamine in the stomach and increased H3K9me3 and H3K27me3 expression, which promoted the proliferation and migration of gastric epithelial cells. Additionally, α-KG reversed this effect. GGT increased the tumorigenic ability of nude mice. GGT, secreted by *H. pylori,* promoted the expression of ribosomal protein L15 (RPL15), while *GGT* knockout and supplementation with α-KG and trimethylation inhibitors reduced RPL15 expression and Wnt signaling pathway expression.

Conclusions *H. pylori* secreted GGT decreased the expression of glutamine and α-KG in gastric epithelial cells, increased the expression of histones H3K9me3 and H3K27me3, and activated the Wnt signaling pathway through RPL15 expression, ultimately changing the biological characteristics of the gastric epithelium and promoting the occurrence of gastric cancer. Altered energy metabolism and histone hypermethylation are important factors involved in this process.

†Xin Jiang and Weijun Wang contributed equally to this work and share first authorship.

*Correspondence:
Rong Lin
linrong@hust.edu.cn
Full list of author information is available at the end of the article

© The Author(s) 2024. **Open Access** This article is licensed under a Creative Commons Attribution-NonCommercial-NoDerivatives 4.0 International License, which permits any non-commercial use, sharing, distribution and reproduction in any medium or format, as long as you give appropriate credit to the original author(s) and the source, provide a link to the Creative Commons licence, and indicate if you modified the licensed material. You do not have permission under this licence to share adapted material derived from this article or parts of it. The images or other third party material in this article are included in the article's Creative Commons licence, unless indicated otherwise in a credit line to the material. If material is not included in the article's Creative Commons licence and your intended use is not permitted by statutory regulation or exceeds the permitted use, you will need to obtain permission directly from the copyright holder. To view a copy of this licence, visit http://creativecommons.org/licenses/by-nc-nd/4.0/.

Keywords Gamma-glutamyl transferase, Alpha-ketoglutarate, Methylation, Energy metabolism, *Helicobacter pylori*, Wnt/β-catenin

Graphical abstract

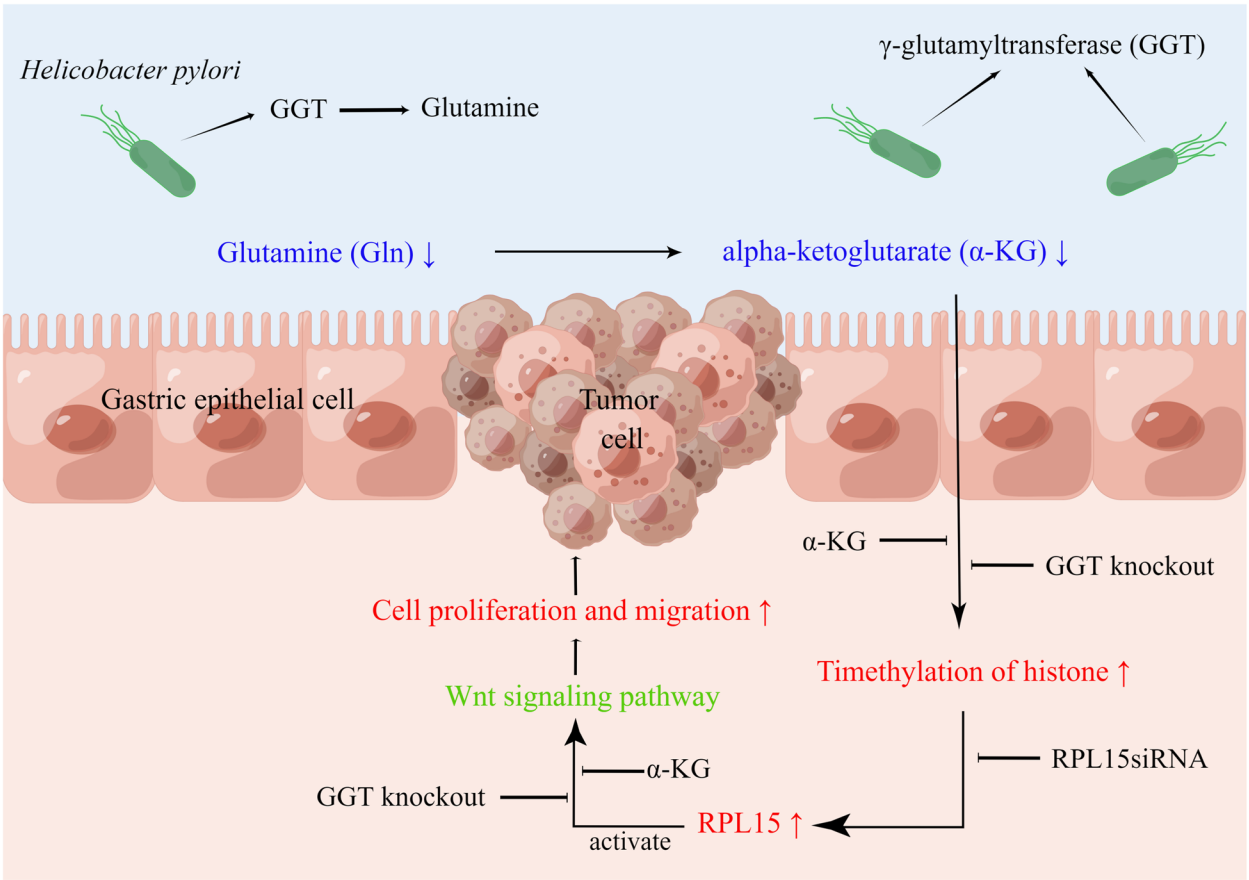

Background

Gastric cancer is the fifth most commonly diagnosed cancer and the third leading cause of cancer death worldwide [1]. *Helicobacter pylori* (*H. pylori*) is recognized as a tier 1 carcinogen by the International Agency for Research on Cancer [2]. Gamma-glutamyl transferase(GGT), a bacterial virulence factor secreted by *H. pylori*, assists it in colonizing the stomach and damaging the gastric epithelium [3, 4]. Our previous studies have revealed that GGT can affect the biological characteristics of mesenchymal stem cells (MSC) by affecting their energy metabolism and methylation state. However, the biological characteristics of gastric epithelial cells remain unclear; therefore, in this study we aimed to explore this aspect in depth [5].

GGT consumes glutamine and glutathione in the gastric environment to provide energy for the growth of *H. pylori*, thereby reducing the concentration of glutamine in the stomach and limiting its the availability for metabolism in gastric epithelial cells [4, 6]. Glutamine can be metabolized into alpha-ketoglutarate (α-KG), to facilitate the tricarboxylic acid (TCA) cycle, thereby regulating the cell fate in adult tissues [6–8]. Exogenous glutamine supplementation significantly alleviates the pathological conditions of the gastric epithelium in mice infected with *H. pylori* [9]. α-KG is mainly derived from glutamine metabolism and is involved in a variety of metabolic and cellular pathways; it affects the function of enzymes that modify chromatin epigenetics (including histone demethylation) and acts as a signaling molecule [10, 11]. A previous study demonstrated that α-KG supplementation maintained low H3K27me3 levels in H3.3K27M mutated cells in diffuse intrinsic

pontine gliomas [12]. Furthermore, in epidermal stem cells, α-KG induceds stem cell differentiation, affects the repressive histone mark H3K27me3, and inhibits tumor initiation and progression [13]. Additionally, MSCs treated with *H. pylori* supernatant showed decreased levels of α-KG metabolites, increased expression levels of H3K9me3 and H3K27me3, and improved the ability of MSCs to proliferate and migrate. Another study revealed that *H. pylori*-induced changes were reversed by adding α-KG [5]. Aberrant DNA methylation of promoter CpG islands can promote the development of gastric and colorectal cancers [14]. Therefore, we hypothesized that *H. pylori* secreted GGT might affect energy metabolism by depleting glutamine and α-KG levels in host cells, thus affecting related histone methylation changes in these cells. However, the specific molecules that affect the biological characteristics of cells require further study.

The Wnt/β-catenin pathway regulates embryonic development and adult tissue homeostasis; the abnormal activation of this pathway can lead to uncontrolled cell growth and malignant transformation [15, 16], which is prominent in the development of gastric cancer associated with *H. pylori* [17, 18]. Depletion of environmental glutamine enhances Wnt signaling in mutant intestinal organoids, while reduced intracellular α-KG levels lead to adenocarcinoma formation in vivo. Histone hypomethylation can lead to the downregulation of Wnt target genes, whereas, glutamine or α-KG supplementation can reduce histone methylation, inhibiting Wnt signaling and tumor growth [19, 20]. Therefore, energy metabolism affects the Wnt signaling pathway.

In summary, the present study investigated the role of GGT secreted by *H. pylori* on the biological characteristics of gastric epithelial cells. We speculated that GGT is involved in tumorigenesis by interfering with glutamine and α-KG metabolism, affecting histone methylation of gastric epithelial cells, activating the Wnt signaling pathway, and improving cell proliferation and migration of the infected cells.

Methods

Animals

Four-week-old male wild-type BALB/c mice were purchased from Beijing Huafukang Biotechnology Co., Ltd.. No female mice were obtained to eliminate the influence of female mouse hormones. The animals were raised in a specific pathogen-free (SPF) laboratory with ad libitum access to food and water. All experimental procedures were performed in accordance with the requirements of the Animal Ethics Committee of the Tongji Medical College, Huazhong University of Science and Technology.

Construction of *GGT* knockout *H. pylori*

The specific construction method used has beenpreviously reported [5]. A mixture of *H. pylori* strain 26695 and plasmid DNA was subjected to 600 Ω resistance, 25 μF capacitance, and 2.5kv Bio-Rad pulse. It was subsequently electrically rotated at -20 ℃ with a gap of 0.2 cm. Current was applied to the mixture with a single 12.5 ms pulse. Kanamycin was used as a screening factor to induce the growth of transformants on the selective medium. The *GGT* knockout *H. pylori* strain was named Hp-KS-1.

Animal gastric cancer model

After one week of acclimated growth in the SPF laboratory, the male BALB/c mice were intragastrically administered antibiotics to remove intragastric bacteria. Each mouse was given ampicillin(5 mg), azithromycin (5 mg), and gentamicin (0.6 mg) daily and were fasted for 4–6 h before antibiotic administration. After 3 days of antibiotic administration, each mouse was administered *H. pylori* by daily gavage (6×10^8 CFU/mL, 0.1 mL/mouse) once every other day for a total of three times. The mice were fasted for 4–6 h before gavage and then fed for 18 months to establish the gastric cancer models.

Cell culture

Human gastric epithelial cell line GES-1 was purchased from Zhong Qiao Xin Zhou Biotechnology Co.,Ltd (ZQ0905, Shanghai, China). Human gastric cancer cell line HGC-27 was purchased from Servicebio (STCC10403P, Wuhan, China). Cells were cultured in a cell incubator containing 5% CO_2 using RPMI-1640 (Gibco, Waltham, MA) medium containing 10% fetal bovine serum (Gibco).

H. pylori culture and cell co-culture system

This specific experimental method has been previously validated by our research group [5, 21]. Liquid medium was prepared by dissolving 3.85 g *H. pylori* medium powder (Qingdao Haibo Biotechnology Co., LTD, Shangdong, China) into 93 mL double distilled water. It was autoclaved and sterilized at 121 °C for 25 min. Next, 7 mL of fetal bovine serum and 1% *H. pylori* selective antibiotics (Qingdao Haibo Biotechnology Co., LTD.) were added to make *H. pylori* medium containing 7% fetal bovine serum. The frozen *H. pylori* 26695 and *GGT* knockout *H. pylori* 26695 strains were thawed and successively added to the prepared *H. pylori* medium. The *H. pylori* strains were incubated for 12 to 16 h at 37 °C and 200 rpm/min in a microaerobic environment (5% O_2, 10% CO_2, and 85% N_2) generated by a microaerobic bag (C-02, Mitsubishi, Japan). The *H. pylori* concentration was determined

by measuring the optical density (OD) at 620 nm. The supernatant OD value for cell experiments measured were all 0.7. The supernatant was subsequently pooled in a centrifuge at 4000 g for 15 min, filtered using a 0.22 micron strainer and frozen at -20 °C. The groups treated with *H. pylori* supernatant or GGT knockout *H. pylori* supernatant were named as the Hp group and Hp-KS-1 group, respectively. We describe the co-culture of cells in detail in the "Cell intervention and grouping" section.

Bacterial DNA collection and 16SRNA sequencing

The gastric tissues of mice in the Hp, Hp-KS-1, and Hp + α-KG groups were ground into homogenates, and 100 μL of the homogenate was inoculated in Columbia blood AGAR medium, (Qingdao Haibo Biotechnology Co., LTD.) which is rich in 7% sterile defibrinated sheep blood. The culture medium was supplemented with antibiotics (vancomycin 10 mg/L, trimethoprim 5 mg/L, cefsulodin 5 mg/L, and amphotericin B 5 mg/L). The inoculated culture plates were incubated at 37 °C in a microaerobic environment (5% O_2, 10% CO_2, and 85% N_2) generated by microaerobic bags (C-02, Mitsubishi, Japan) for 3 to 7 days to form visible bacterial colonies. Genomic DNA was isolated from the bacteria using a Bacterial Genomic DNA Extraction kit (DP302, TianGen, Beijing, China) according to the manufacturer's recommendations. Then, primers 27F 5 ′-AGTTTGATCMTGGCTCAG-3′ and 1492R 5 ′-GGTTACCTTGTTACGACTT-3′ were used to amplify the conserved region of 16S rRNA. After the polymerase chain reaction (PCR), its products were determined by 1% agarose gel electrophoresis, the target band was cut and purified, and the recovered products were used for Sanger sequencing. Sequencing results were analyzed using the ContigExpress software (Thermo Fisher Scientific), and compared with the NCBI database (https://blast.ncbi.nlm.nih.gov/Blast.cgi) for *H. pylori* species identification.

Metabolite detection

Glutamine (BioVision, Milpitas, CA) and α-KG (BioVision) kits were used to detect the content of glutamine and α-KG, respectively. The metabolites were analyzed according to the experimental procedure.

Cell intervention and grouping

GES-1 and HGC-27 cells were collected and resuspended in complete medium and seeded in six-well plates at a density of 2×10^4 cells/mL. When the cells grew to an 80–90% density, *H. pylori* supernatant or Hp-KS-1 supernatant was incubated with gastric cells for 12 h at a final dilution of 1:35 and divided into *H. pylori* group and Hp-KS-1 group. Cells in the α-KG group were simultaneously treated with *H. pylori* supernatant (incubated with gastric cells at a final dilution of 1:35) and dimethyl-α-ketoglutarate (349631, Sigma-Aldrich, St. Louis, MO), diluted to a concentration of 5 mM with dimethyl sulfoxide for 12 h at the same time. The addition value of dimethyl-α-ketoglutarate have been applied in the previous research results of our group and were confirmed in this study [5].

In this study, the control group consisted of cells cultured in RPMI-1640 medium alone, while the Hp and Hp-KS-1 groups consisted of cells treated with *H. pylori* supernatant and Hp-KS-1 supernatant, respectively. The α-KG group consisted of cells treated simultaneously with *H. pylori* supernatant and dimethyl-α-ketoglutarate. The methylation inhibition group consisted of cells treated with 100 nM BIX01294 (S8006, Selleck Chemicals, Houston, TX) and 2 μM GSK126 (S7061, Selleck Chemicals) for 72 h.

Cell immunofluorescence

The 24-well plates were carefully wetted with phosphate buffered saline (PBS) to remove excess liquid. The coverslips were carefully placed in the 24-well plate to prevent bubble formation. The cell medium was aspirated and the cells on the coverslips were washed with PBS. The cells were then fixed with 4% paraformaldehyde, perforated with 0.3% Triton, and subsequently blocked with 1% donkey serum blocking solution for 30 min to 1 h. After that, the primary antibody β-catenin (1:200 dilution) (Additional file 2: Table S1) diluted in PBS was incubated at 4 ℃ overnight. After rewarming on the next day, the slides were co-incubated with the secondary antibody (1:200 dilutions), diluted in PBS for 1 h (protected from light), and the excess antibody was washed with PBS. Nuclei were stained with Hoechst-33258 at 1 μg/mL for 8 min, and excess antibody was washed away with PBS. Finally, the slides were sealed with an anti-quenching agent, and the results were observed under an Olympus BX53 fluorescence microscope (Olympus Life Science, Waltham, MA) using the CellSens Dimension software (Olympus Life Science).

Tissue immunofluorescence

Paraffin sections were routinely dewaxed to hydration, and after antigen repair, membranes were broken with 0.3% Triton for 15–30 min and blocked with 1% donkey serum blocking solution for 30 min to 1 h. Primary antibody β-catenin (1:200 dilution) diluted in PBS (Additional file 2: Table S1) was incubated overnight at 4 °C. The next day, after rewarming, the secondary antibody (1:200 dilution) was incubated in the dark for 1 h, stained with Hoechst-33258 (DAPI) at 1 μg/mL, and the anti-quenching tablet was blocked. In being future-proof BX53 fluorescence microscope using CellSens Dimension software observations.

Immunohistochemical staining

Immunohistochemical staining was performed on tumor specimens obtained from our mice model or nude mice. Sections were deparaffinized with xylene and absolute ethanol and boiled in citrate buffer. The samples were then cooled in water. The immunohistochemical pen tissue was circled. The H_2O_2 enzyme was inactivated and 0.3% Triton reagent was used to make the antibody more permeable to the cell membrane. Sections were incubated with bovine serum albumin at 37℃ for 30 min. Subsequently, sections were incubated with Ki-67 antibody (D3B5) (#12202, Cell Signaling Technology, Danvers, MA) at a 1:200 dilution. The sections were subjected to nuclear coloration with secondary antibody and DAB, counterstained with hematoxylin, dehydrated, oven-dried, and sealed with resin. The immunohistochemical results were observed under an Olympus BX53 fluorescence microscope using the CellSens Dimension software (Olympus Life Sciences).

CFSE assay

GES-1 cells were digested and counted using a counter plate. The cell concentration was adjusted to $5–10\times10^6$ cells/ml. Negative controls were stored in a 4 ℃ environment using paraformaldehyde fixation. Later, the cells were labeled with 1 mM of the fluorescent dye carboxyfluorescein diacetate succinimidyl ester (CFSE, Vazyme, Nanjing, China). The reaction was terminated, and the excess dye was washed off. The positive control group was fixed and stored at 4 ℃. The remaining cells were grouped and treated according to the experimental requirements, and cell proliferation was detected by flow cytometry.

CCK8 proliferation assay

GES-1 cells were digested, washed, and counted using counter plates. A total of 7000–9000 cells were seeded per well in 96-well plates. After cell adhesion, cells were divided into groups for intervention. Subsequently, 10 μL of CCK8 solution was added to each well. Cell proliferation was observed by measuring the absorbance at 450 nm.

Colony-forming experiment

GES-1 cells were harvested and resuspended in complete medium and seeded in 6-well plates at a density of 500 to 1,000 cells per well. After the cells were placed in the cell incubator for 12 h, cells were grouped and intervened according to the experimental requirements. The medium was then changed every 2 days and the cells were observed microscopically until visible colonies of at least 50 cells were formed. Cells from all groups were washed thrice with PBS, fixed with 4% paraformaldehyde for 30 min, and stained with 0.5% crystal violet for 15 min. Finally, all cell colonies were counted using the light counting method after the cells were washed with PBS again to analyze cell proliferation.

EdU cell proliferation assay

GES-1 cells were collected and seeded at 2×10^4 cells/well in 24-well plates covered with cell slides. After cells were cultured overnight and returned to the normal state, *H. pylori* supernatant and α-KG were used for intervention. The prepared 20 μM EdU 2×working solution was added to the 24-well plate with an equal volume of culture medium to change the final EdU concentration in the 24-well plate to 10uM and incubated for an additional 2 h. After that, the cells were fixed, washed, and permeabilized with PBS containing 0.3% Triton X-100. The cells were reacted with the cell proliferation Detection kit (C0071 BeyoClick™EdU-488, Beyotime Biotechnology, Jiangsu, China). Hoechst 33342 was used for nuclear staining, and finally cell slides were sealed with anti-quencher. Fluorescence was observed under an Olympus BX53 fluorescence microscope using the CellSens Dimension software (Olympus Life Sciences).

Transwell experiment

In Transwell plates (pore size, 8 μM; Corning Inc., Corning, NY), the upper chamber was seeded with 1×10^4 GES-1 cells and 200 μL of serum-containing medium was added. A volume of 600 μL of serum-containing medium was added to the lower chamber. After the cells adhered to the wall, the medium in the lower chamber was replaced, and *H. pylori* supernatant and α-KG were added according to the grouping. After 48 h, the samples were collected, observed under a microscope, and photographed.

Wound healing

GES-1 cells were spread in 12-well plates, and cell scratches were created with 200 μL of the tip of the gun, rinsed with PBS, and examined under an Olympus microscope (Olympus Life Sciences). The cells were then treated with *H. pylori* supernatant and α-KG in 12-well plates for 24 h and their migration status was observed and photographed. Migration was measured based on the size of the wound healing area.

Extraction of protein

Cells or mouse tissues were harvested, cells were lysed in RIPA lysate (1% PMSE), and protein quantification was achieved by using the BCA Protein Assay Kit (Vazyme). Nuclear protein extraction reagent (Solarbio, Beijing, China) was used to extract nuclear proteins according to the experimental procedure. After denaturation at 100 ℃, storage at -80 ℃, further operations were carried out.

Western blotting

Loading was performed at 40 μg mass and proteins were separated by SDS-PAGE polyacrylamide gel

Table 1 Sequences of primers used for real-time quantitative PCR

Genes	Forward primer 5′-3′	Reverse primer 5′-3′
mRPL15	**GTCCGCTGTTGGCAATACC**	**ACATAGCCTTGCTTAGCCTTGTA**
hRPL15	**CCAGCTAAAGTTTGCTCGAAG**	**GACTCTCAGAGCCCCACAGT**
mAxin2	**TGACTCTCCTTCCAGATCCCA**	**TGCCCACACTAGGCTGACA**
hAxin2	**TACACTCCTTATTGGGCGATCA**	**TTGGCTACTCGTAAAGTTTTGGT**
mCyclin D1	**CTCCGTATCTTACTTCAAGTGCG**	**CTTCTCGGCAGTCAAGGGAA**
hCyclin D1	**CTGTGCTGCGAAGTGGAAACCAT**	**TTCATGGCCAGCGGGAAGACCTC**
mc-Myc	**ATGCCCCTCAACGTGAACTTC**	**CGCAACATAGGATGGAGAGCA**
hc-Myc	**TGGTCTTCCCCTACCCTCTCAAC**	**GATCCAGACTCTGACCTTTTGCC**
mGAPDH	**CTTCATTGACCTCAACTACATGGTCTA**	**GATGACAAGCTTCCCATTCTCAG**
hGAPDH	**GACAGTCAGCCGCATCTTCT**	**TTAAAAGCAGCCCTGGTGAC**

electrophoresis. After electrophoresis, proteins on the gel were transferred to polyvinylidene difluoride membranes and then blocked using a rapid blocking solution. The bands and specific antibodies (all 1:1000 dilutions) (Additional file 2: Table S1) used were: H3K9me3 (A2360, Abclonal, Woburn, MA), H3K27me3 (A2363, Abclonal), H3K9me1 (A2358, Abclonal), H3K27me1 (A2361, Abclonal), H3 (A2348, Abclonal), β-catenin (8480, CST), transcription factor 4 (TCF4) (2569, Cell Signaling Technology), secreted frizzled related protein 1 (SFRP1) (A2911, Abclonal), RPL15 (A3241, Abclonal), and β-actin (AC026, Abclonal). These antibodies were incubated at 4℃ overnight. This was followed by incubation with HRP-conjugated second antibody (1:1000 dilutions) at room temperature, and finally the protein bands were visualized using enhanced chemiluminescence (Vazyme).

RNA Extraction and real-time quantitative PCR

RNA was isolated using the TRIzol reagent (Vazyme), and the concentration was measured using a spectrophotometer. Real-time quantitative PCR (RT-qPCR) was performed and transcribed into cDNA using the Vazyme Synthesis Kit. RT-qPCR was performed using the StepOne Real-time PCR system (Applied Biosystems, Waltham, MA) and normalized to GAPDH using the $2^{-\Delta CT}$ method. The primer sequences are listed in Table 1.

Small interfering RNA (siRNA) transfection

The Wuhan Qing branch Co., Ltd. (Wuhan, China) designed and synthesized the target RPL15 siRNA and the negative control (NC) siRNA. The sequence of RPL15 siRNA was as follows: sense: 5′-CAAGCAAGGUUACGUUAUATT-3′, antisense: 5′-UAUAACGUAACCUUGCUUGTT-3′.

Transfection was performed 24 h before transfection by seeding $0.5–2\times10^{5}$ GES-1 cells in 24-well plates (Corning Inc.) containing 400 μL of antigen-free medium/well at 60 to 80% cell confluence. siRNA was diluted to a concentration of 20 μM in Opti-MEM (Thermo Fisher Scientific, Waltham, MA). The transfection reagent Lipofectamine® 3000 (Invitrogen, Waltham, MA) was similarly diluted in Opti-MEM at a transfection concentration of 50 nM. Diluted siRNA was mixed with transfection reagent and transfected into cells seeded in 24-well plates. After 4–6 h, fresh medium was replaced, and transfection was continued for another 24 h for subsequent experiments.

Tumor formation in nude mice

All animal experiments were approved by the Medical Ethics Committee of Wuhan Union Hospital. Four-week-old Balb/c male nude mice (Beijing Hufukang Biotechnology Co., LTD., Beijing, China) were placed in a specific

(See figure on next page.)

Fig. 1 The ability of gamma-glutamyl transferase secreted by *H. pylori* to promote the proliferation and migration of gastric epithelial cells. **A** Representative images and statistical analysis of Ki-67 immunohistochemical staining in gastric tissues of control, Hp, and Hp-KS-1 mice ($n=5$ per group). **B** Proliferation of gastric epithelial CFSE cells in the control, Hp, and Hp-KS-1 groups and the statistical analysis. **C** Cell cloning results and statistical analysis of gastric epithelial cells in the control, Hp, and Hp-KS-1 groups. **D** EdU cell proliferation results of gastric epithelial cells in the control, Hp, and Hp-KS-1 groups and the statistical analysis. **E** CCK8 assay of gastric epithelial cells in the control, Hp, and Hp-KS-1 groups. **F** Transwell cell migration results of gastric epithelial cells in the control, Hp, and Hp-KS-1 groups and the statistical analysis. **G** Wound healing test results of gastric epithelial cells in the control, Hp, and Hp-KS-1 groups and the statistical analysis. Data are expressed as mean ± standard deviation. * $p<0.05$, * *$p<0.01$, * * * $p<0.001$, * * * *$p<0.0001$. Abbreviations: GES-1: human gastric epithelial cell line; Hp: *H. pylori* intervention group; Hp-KS-1: gamma-glutamyl transferase knockout *H. pylori* intervention group; CFSE: Fluorescent label carboxyfluorescein diacetate succinimidyl ester; CCK8: Cell Counting Kit-8; EdU: 5-ethynyl-2 ′-deoxyuridine; Ki-67 relative ratio: Relative size of Ki-67 positive area in immunohistochemistry of each group; M1%: Proportion of M1 negative in CFSE flow plots; Relative colony number: Relative colony number of cell clones in each group

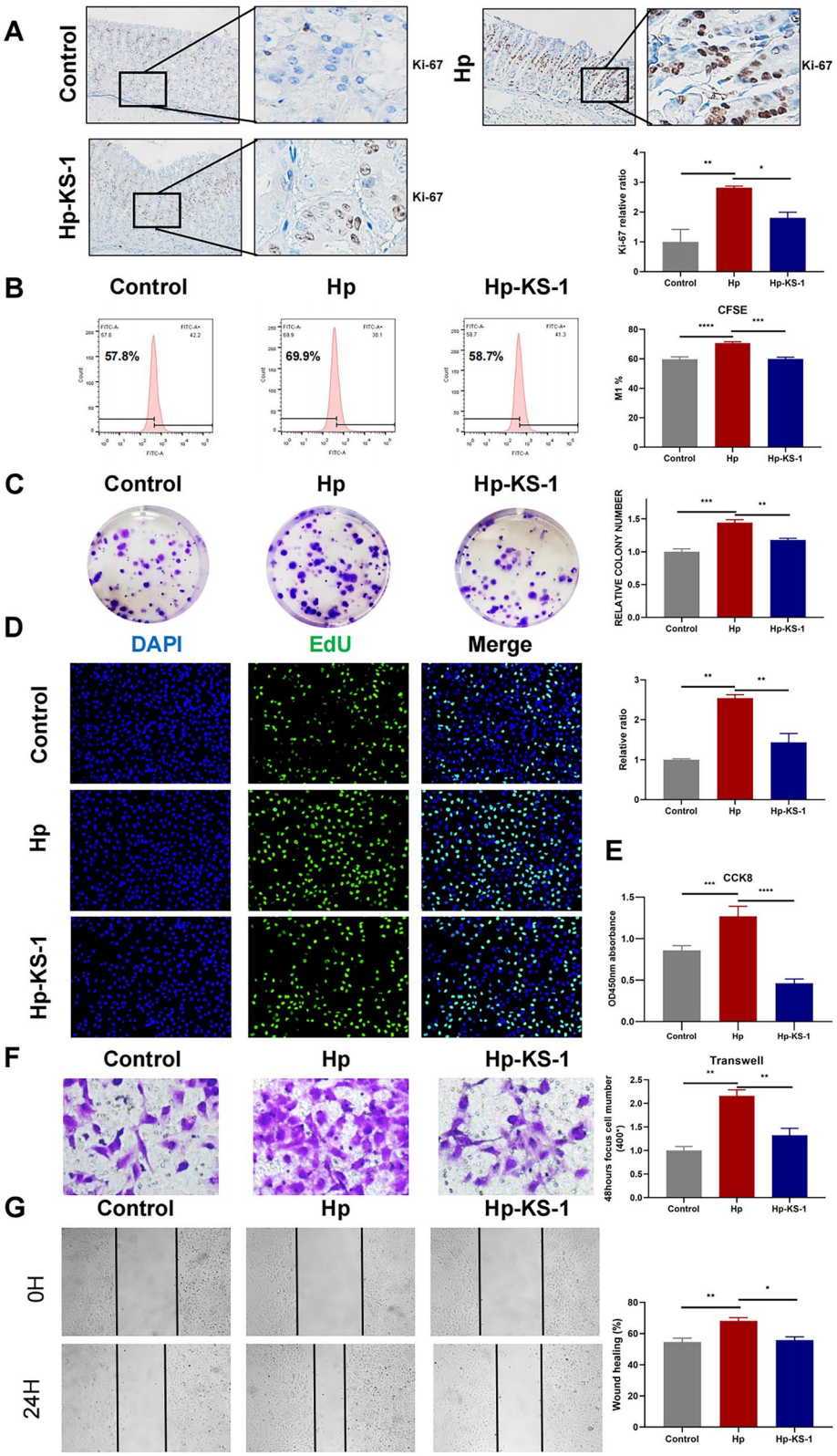

Fig. 1 (See legend on previous page.)

pathogen-free environment. *H. pylori* supernatants or Hp-KS-1 supernatants were incubated with HGC-27 gastric cancer cells at a final dilution of 1:35 as described above. *H. pylori* supernatant supplemented with 5 mM α-KG was incubated with HGC-27 gastric cancer cells at a final dilution of 1:35. Subsequently, the cells in different groups were diluted to 1×10^{7} cells/mL with PBS and injected into the right subcutaneous area of mice at a dose of 200 μL. The animal models were divided into control, Hp + HGC-27, Hp-KS-1 + HGC-27, and Hp + α-KG + HGC-27 groups. Tumor formation, was measured after every 3 days using a vernier caliper to determine subcutaneous tumor length (L) and width (W), calculated by the formula $(L\times W^2)\times0.5$ tumor volume. Mice were euthanized 4 weeks later, and the tumor biopsy specimens were analyzed.

Statistical analysis

SPSS 23.0 (IBM Corp., Armonk, NY), GraphPad Prism 8.0 (GraphPad Software, La Jolla, CA), and ImageJ software (National Institutes of Health, Bethesda, MD) were used for statistical analyses and drawings. All experimental data are presented as mean ± standard deviation. An independent sample t-test was used for comparisons between the two groups. Analysis of variance (ANOVA) was used to compare multiple groups. $P<0.05$ was considered statistically significant.

Results

GGT of *H. pylori* increased the proliferation and migration of gastric epithelial cells

Mice were intragastrically administered with cultured *H. pylori* or *GGT* knockout *H. pylori* (Hp-KS-1) for 18 months. Bacteria in gastric tissues of mice were collected and cultured for 16sRNA sequencing. The sequencing results were compared with the NCBI database, and it was found that the nucleic acid base sequence with *H. pylori* 26695 was more than 99% identical, which confirmed the continuous colonization of *H. pylori* in the gastric tissue of mice (Additional file 1: Figure S 1A). The mice gastric tissues were stained with hematoxylin and eosin and pathological changes were observed under a microscope. No obvious abnormal changes were found in the stained sections of the control group, whereas the gastric mucosal surfaces of the mice treated with *H. pylori* showed mucosal exfoliation and nuclear polarity changes, which are manifestations of dysplasia. Hematoxylin and eosin-stained sections of the *GGT* knockout *H. pylori* group showed reduced glands with mild atrophy. Ki-67 immunohistochemical staining was performed on gastric tissue sections of mice, and the *H. pylori* group showed the highest Ki-67 expression ($P<0.05$), indicating the most vigorous proliferation. The expression was weaker in the Hp-KS-1 group than the *H. pylori* group (Fig. 1A).

Gastric epithelial cells were treated with either *H. pylori* supernatant or Hp-KS-1 supernatant, and changes in the biological characteristics of gastric epithelial cells were observed. Through CFSE, CCK8, cell cloning, and EdU experiments (Fig. 1B-E), it was found that the proliferative ability of cells in the *H. pylori* group was significantly enhanced, while it was partially reversed in the Hp-KS-1 group.

To examine the effect of GGT on cell migration, transwell and cell scratch assays were performed (Fig. 1F-G). GGT secreted by *H. pylori* promoted cell migration; accordingly, the transwell assay showed that *H. pylori* supernatant had the highest cell migration ability compared to the other groups. This result was confirmed using a cell scratch assay.

GGT secreted by *H. pylori* induces low glutamine and α-KG microenvironment, which increases the proliferation and migration ability of gastric epithelial cells

GGT is an essential enzyme in *H. pylori* that is closely associated with the consumption of glutamine (GLN). Changes in GLN may alter the content of the TCA cycle intermediate substance α-KG in gastric epithelial cells. Therefore, in order to further confirm whether *H. pylori* secreted GGT could change the biological characteristics of gastric epithelial cells by regulating the α-KG content, we added α-KG to GES-1 treated with *H. pylori* medium supernatant. The GES-1 metabolites GLN and α-KG were quantified using the corresponding detection kits.

(See figure on next page.)

Fig. 2 Secretion of gamma-glutamyl transferase by *H. pylori* reduced the content of glutamine and α-KG, and the ability of proliferation and migration of gastric epithelial cells was weakened after α-KG supplementation. **A** Glutamine levels were determined in the control, Hp, and Hp-KS-1 groups. **B** α-KG levels in the control, Hp, and Hp-KS-1 groups. **C** Representative images and statistical analysis of Ki-67 immunohistochemical staining in gastric tissues of mice from the Hp and α-KG (Hp + α-KG) supplementation groups. **D** CFSE cell proliferation results and statistical analysis of the Hp and α-KG (Hp + α-KG) supplementation groups. **E** Cloning results and statistical analysis of the Hp and α-KG (Hp + α-KG) supplementation groups. **F** CCK8 cell proliferation assay results of the Hp and α-KG (Hp + α-KG) supplementation groups. **G** EdU cell proliferation in the Hp and α-KG (Hp + α-KG) supplementation groups and the statistical analysis. **H** Transwell cell migration results and statistical analysis of the Hp and α-KG (Hp + α-KG) supplementation groups. **I** Wound healing test results and statistical analysis of the Hp and α-KG (Hp + α-KG) supplementation groups. Data are expressed as mean ± standard deviation. *$p<0.05$, **$p<0.01$, ***$p<0.001$. Abbreviations: CCK8: Cell Counting Kit-8; CFSE: Fluorescent label carboxyfluorescein diacetate succinimidyl ester; EdU: 5-ethynyl-2 '-deoxyuridine; Hp: *H. pylori* intervention group; Hp-KS-1: gamma-glutamyl transferase knockout *H. pylori* intervention group

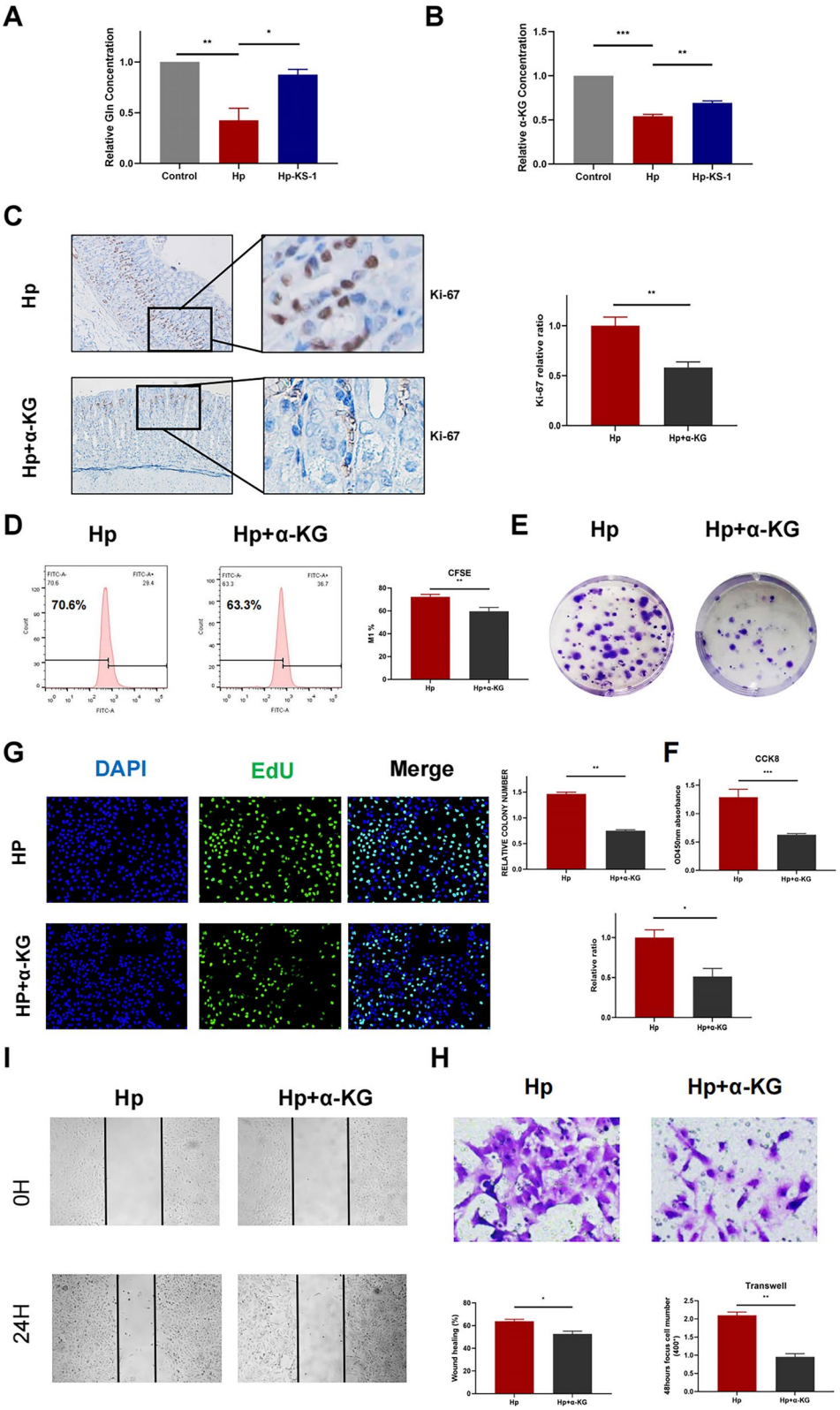

Fig. 2 (See legend on previous page.)

The results showed that the contents of GLN and α-KG in *H. pylori* group were significantly decreased ($P < 0.05$), and the decrease in Hp-KS-1 group was smaller than that in *H. pylori* group (Fig. 2A-B).

After 2 months of *H. pylori* intragastric administration, the mice were fed regular drinking water containing α-KG for 16 months, which was designated as the α-KG supplementation group. The results of bacterial 16sRNA sequencing in mouse gastric tissues also confirmed the persistent colonization of *H. pylori* in mouse gastric tissues. (Additional file 1: Figure S 1A). Ki-67 immunohistochemical staining in gastric tissue sections of mice in the *H. pylori* and α-KG supplementation group showed that the proliferation of *H. pylori* was significantly higher in the *H. pylori* group than in the α-KG supplementation group (Fig. 2C).

The results of the proliferation and migration experiments showed that the proliferation and migration abilities of the *H. pylori* group were significantly enhanced. Compared to the *H. pylori* group, the biological characteristics of proliferation and migration in the α-KG supplementation group were weakened (Fig. 2D-I).

GGT secreted by *H. pylori* may affect the energy metabolism of gastric *cancer* cells and participate in the development of gastric cancer

To further explore the correlation between the effect of GGT on energy metabolism and the occurrence of gastric cancer, tumors were established in nude mice. HGC-27 gastric cancer cells alone, as well as HGC-27 gastric cancer cells treated with *H. pylori* supernatant, Hp-KS-1 supernatant, and *H. pylori* supernatant with α-KG were injected subcutaneously into nude mice. After 4 weeks of observation, the tumor volume was recorded, and the tumors of the nude mice in each group were weighed. The results showed that the weight and volume of the tumors in the *H. pylori* group, as well as the growth rate, were significantly higher than those in the other groups (Fig. 3A-D). Gastric cancer tumor growth was partially reversed after α-KG supplementation. Ki-67 immunohistochemical staining of tumor tissue sections also showed that the *H. pylori* group had the most vigorous proliferation (Fig. 3E). These results suggest that GGT secreted by *H. pylori* may promote the proliferation of gastric cancer cells by reducing the α-KG content, thereby promoting the occurrence of gastric cancer.

GGT secreted by H. pylori affects the content of α-KG in gastric epithelial cells, thereby affecting the histone methylation status of gastric epithelial cells

The mechanism by which α-KG affects cell proliferation and migration remains unexplored. Some studies have reported that α-KG is closely related to histone methylation in cells, and histone methylation regulates cell growth. In order to explore the effect of α-KG on the proliferation and migration of gastric epithelial cells, we performed in vitro and in vivo testing.

In vitro, *H. pylori* supernatant, Hp-KS-1 supernatant and α-KG-supplemented *H. pylori* supernatant were used to treat gastric epithelial cells. For in vivo experiments, we selected the corresponding groups. The nuclear proteins were extracted to detect histone methylation. The results showed that the expression of H3K9me3 and H3K27me3 increased, and the expression of H3K9me1 and H3K27me1 decreased in *the H. pylori* group. Compared to the *H. pylori* group, the Hp-KS-1 group showed less trimethylation of H3K9 and H3K27. However, α-KG supplementation downregulated the expression levels of H3K9me3 and H3K27me3 (Fig. 4A-B). These results indicated that α-KG, a metabolite of energy metabolism, could modify the methylation status of histones under the influence of GGT.

GGT secreted by H. pylori affects RPL15 expression

To further explore the downstream changes in energy metabolism affected by GGT, gastric tissues of mice in the *H. pylori* and GGT knockout *H. pylori* groups were collected for proteomic sequencing. Gene ontology analysis revealed that differentially expressed proteins were clustered mainly in the ribosomal part (Fig. 5A). Volcano plot analysis showed that the ribosomal protein RPL15 expression was significantly lower in Hp-KS-1 group than in the *H. pylori* group (Fig. 5B), ($P < 0.05$). RPL15 is the most critical ribosomal protein in carcinogenesis and overexpression of RPL15 increases the risk of tumor formation [22]. PCR analysis of tissues and cells from *H.*

(See figure on next page.)

Fig. 3 *H. pylori* increased the tumor formation ability in nude mice, which was weakened after α-KG supplementation. **A**-**B** Tumor formation images of nude mice in the HGC-27 only, Hp + HGC-27, Hp-KS-1 + HGC-27, and Hp + α-KG + HGC-27 groups ($n = 3$ in each group). **C**-**D** Statistical analysis of tumor weight and volume in the HGC-27 only, Hp + HGC-27, Hp-KS-1 + HGC-27, and Hp + α-KG + HGC-27 groups ($n = 3$ in each group). **E** Representative images and statistical analysis of Ki-67 immunohistochemical staining in tumor tissues of nude mice in the HGC-27 only, Hp + HGC-27, Hp-KS-1 + HGC-27, and Hp + α-KG + HGC-27 groups ($n = 3$ in each group). Data are expressed as mean ± standard deviation. ***$p < 0.001$, ****$p < 0.0001$. Abbreviations: HGC-27: human gastric cancer cell line; Hp + HGC-27: *H. pylori* supernatant-treated gastric cancer cells; Hp-KS-1 + HGC-27: gastric cancer cells treated with Hp-KS-1 supernatant; Hp + α-KG + HGC-27: gastric cancer cells treated with *H. pylori* supernatant supplemented with α-KG

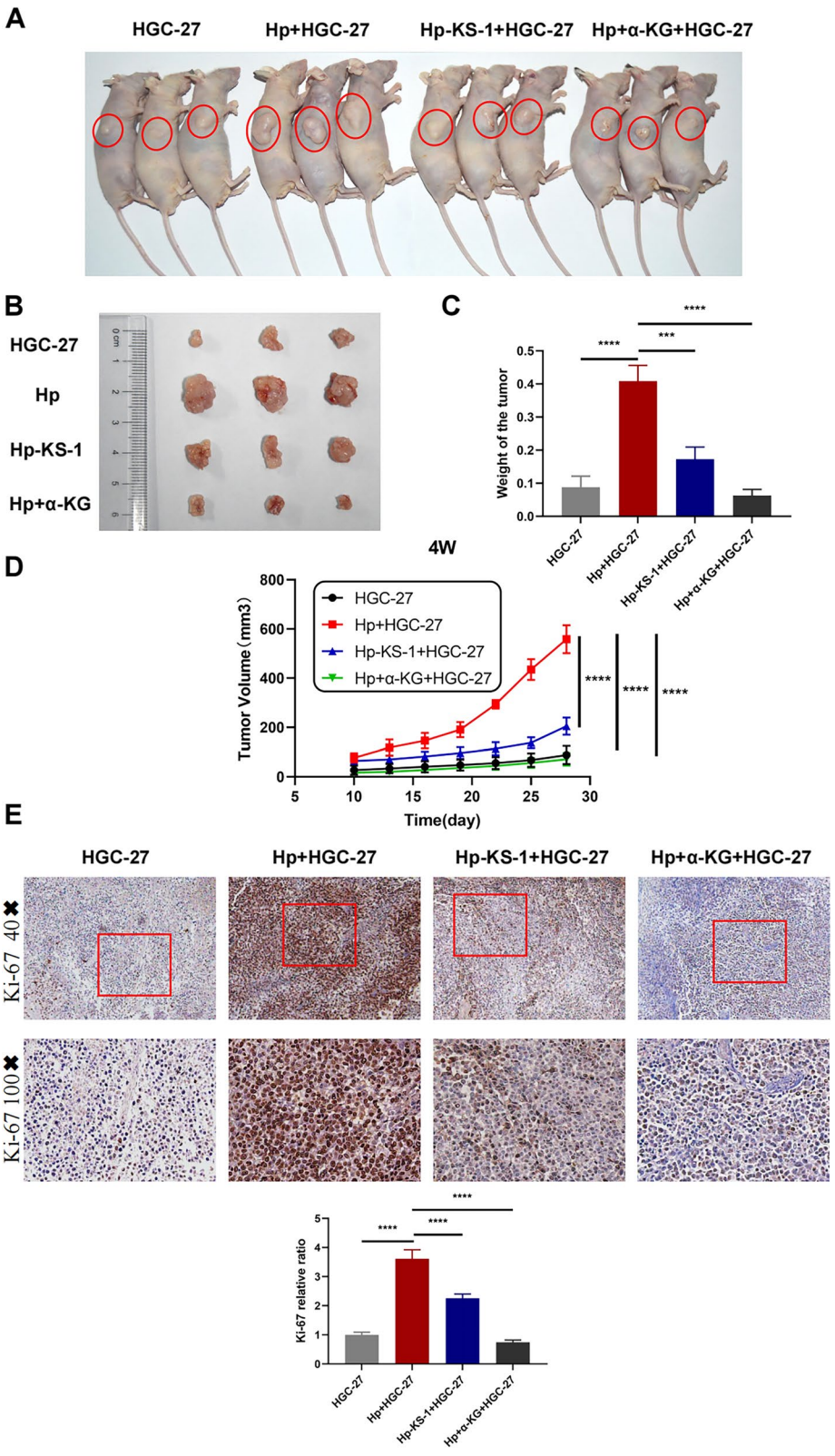

Fig. 3 (See legend on previous page.)

pylori and Hp-KS-1 groups showed that the expression of RPL15 was substantially higher in the *H. pylori* group than in the Hp-KS-1 group, and the Western blotting results were similar (Fig. 5C-D). These results suggest that the expression of RPL15 is related to GGT, and it may be an intermediate molecule affecting energy metabolism and downstream signaling pathways; however, this needs to be further verified.

GGT secreted by H. pylori can affect the energy metabolism and histone methylation status of gastric epithelial cells and the expression of RPL15

PCR and Western blotting were used to detect the expression of ribosomal protein RPL15 in gastric epithelial cells treated with *H. pylori* supernatant, Hp-KS-1 supernatant, and α-KG supplemented *H. pylori* supernatant, as well as in gastric tissues of corresponding mice. Our data indicated that the expression of RPL15 was significantly increased in the *H. pylori* group but decreased in the Hp-KS-1 group, and this high expression was reversed by α-KG supplementation (Fig. 6A-C). To further verify the effect of methylation status on RPL15 expression, we used the combined inhibitors of H3K27 and H3K9 trimethylation, BIX01294 and GSK126, and found that the expression of RPL15 was decreased in the *H. pylori*, Hp-KS-1, and α-KG supplement groups after the addition of trimethylation inhibitors (Fig. 6D). This indicates that GGT affects the energy metabolite α-KG, which in turn influences the methylation status and consequently the expression of RPL15.

GGT secreted by H. pylori can affect α-KG and histone methylation in gastric epithelial cells and activate the Wnt signaling pathway through RPL15

The Wnt signaling pathway regulates body development and its activation promotes the occurrence of gastric cancer. Overexpression of RPL15 selectively upregulates β-catenin, which may be involved in the occurrence of gastric cancer through the Wnt signaling pathway. For further validation, we examined Wnt signaling and transfected GES-1 cells with siRNA to knockdown *RPL15*. β-catenin is normally expressed in the cell membrane and cytoplasm. The translocation of β-catenin into the nucleus usually indicates the activation of Wnt signaling pathway. The results showed that β-catenin was translocated to the nucleus in GES-1 cells under *H. pylori* infection, but not in *RPL15* knockdown cells (Fig. 7A), indicating that RPL15 may be involved in the Wnt/β-catenin signaling pathway. Negative control cells with *H. pylori* supernatant and *H. pylori*-infected RPL15 knockdown gastric epithelial cells were used to detect Wnt signaling pathway-related protein expression. The expression of Wnt signaling pathway-related proteins was increased in the *H. pylori* group compared with RPL15 knockdown groups and the negative control group (Additional file 1: Figure S2A). *H. pylori* in gastric cancer can activate the Wnt signaling pathway; the pathway increases the expression of β- catenin/TCF4-related target genes (cyclin D1, Axin2 and c-Myc) [23, 24]. The above cells were grouped for RT-qPCR detection. The expression of cyclin *D1*, *Axin2* and *c-Myc* were significantly higher in negative control cells treated with *H. pylori* than in the knockdown group (Additional file 1:Figure S 3A). These results suggested that RPL15 could mediate the activation of the Wnt/β-catenin signaling pathway.

In order to explore the relationship between GGT and Wnt signaling pathway activation, the expression of Wnt signaling pathway-related proteins was detected by Western blotting in gastric epithelial cells treated with *H. pylori*, Hp-KS-1 supernatant, and α-KG-supplemented *H. pylori* supernatant, and the gastric tissues of corresponding mice. The results showed that compared with the control group, Wnt signaling pathway-related protein expression were significantly increased and Wnt signaling pathway inhibitor protein expression was significantly decreased in the *H. pylori* treatment group, while the changes in the Hp-KS-1 group were smaller than those in the *H. pylori* group. The α-KG supplement group showed opposite changes (Fig. 7B-C). GES-1 cells and corresponding mouse tissues were collected for RT-qPCR; it was also found that the expression of β-catenin/TCF4 related target genes (cyclin D1, *Axin2* and *c-Myc*) was significantly higher in the *H. pylori* treatment group than in the normal group. Knockout of *GGT* and supplementation of α-KG decreased the expression of these genes (Additional file 1: Figure S3B-C). The nuclear translocation of β-catenin was also observed in GES-1

(See figure on next page.)

Fig. 4 Gamma-glutamyl transferase secreted by *H. pylori* affects energy metabolism and histone methylation status of gastric epithelial cells. **A** Representative images of H3K9me3, H3K27me3, H3K9me1 and H3K27me1 expression in gastric epithelial cells of the control, Hp, Hp-KS-1, and Hp + α-KG groups using Western blot assay and the statistical analysis. **B** Representative images of H3K9me3, H3K27me3, H3K9me1 and H3K27me1 expression in gastric tissues of mice in the control, Hp, Hp-KS-1, and Hp + α-KG groups were detected by Western blot assay and analyzed statistically. Data are expressed as mean ± standard. *$p < 0.05$, **$p < 0.01$, ***$p < 0.001$. Abbreviations: Hp: *H. pylori* intervention group; Hp + α-KG: Hp and α-KG supplementation group; Hp-KS-1: gamma-glutamyl transferase knockout *H. pylori* intervention group

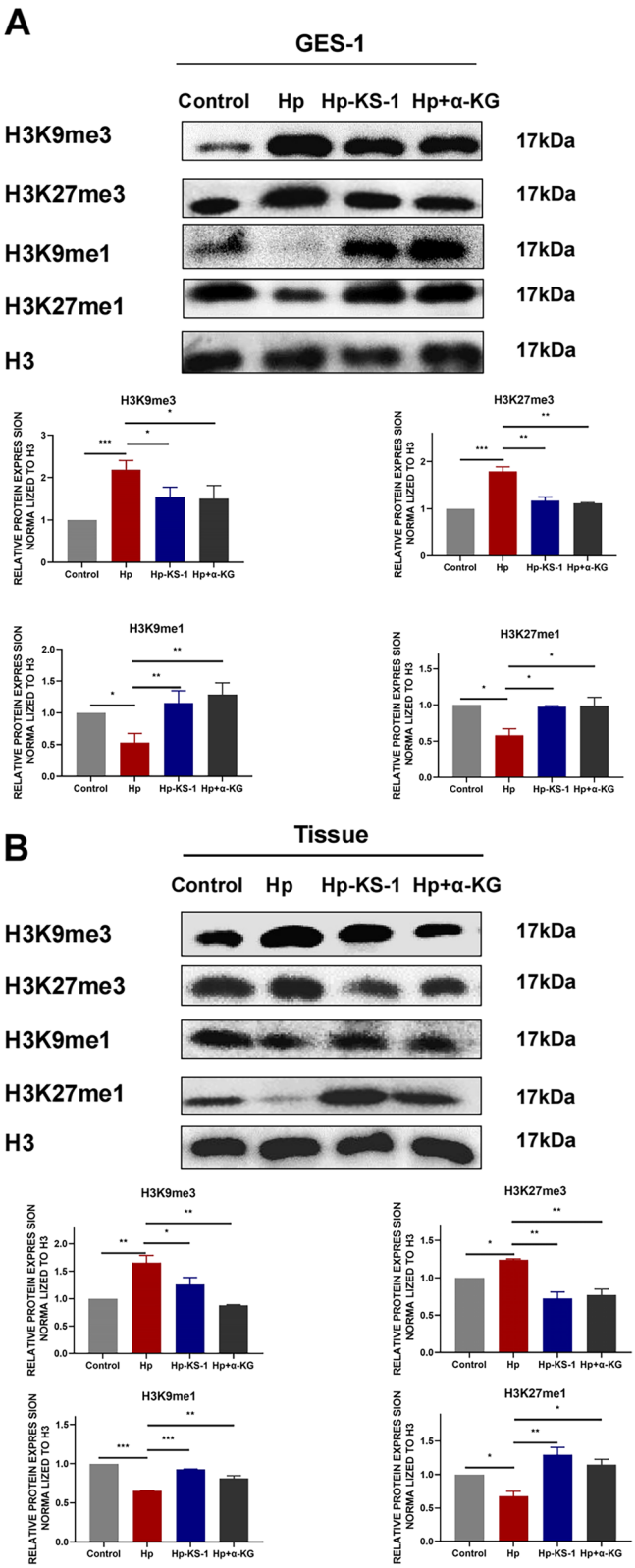

Fig. 4 (See legend on previous page.)

cells and gastric tissues of mice in the *H. pylori* group, but not in the Hp-KS-1 and α-KG supplemented groups (Additional file 1: Figure S4A-B). To verify the effect of histone hypermethylation on the Wnt signaling pathway, combined inhibitors of H3K9 and H3K27 trimethylation (BIX01294 and GSK126, respectively) were added to the cell culture medium. We found that the expression of β-catenin and TCF4 was significantly decreased in the Inhibition group, whereas the expression of SFRP1 was significantly increased (Fig. 7D). Similarly, the expression of cyclin D1, Axin2 and c-Myc was decreased in the inhibition group (Additional file 1: Figure S3D). Ectopic nuclear translocation of β-catenin was not observed (Additional file 1: Figure S4C). These results show that GGT secreted by *H. pylori* affects the energy metabolite α-KG and histone methylation status, thereby modulating the Wnt signaling pathway activation.

To performed further experiments to confirm whether RPL15 is a mediator of α-KG and histone methylation and verify its role in the Wnt signaling pathway. *H. pylori* supernatant, *GGT* knockout *H. pylori* supernatant, α-KG-supplemented *H. pylori* supernatant intervened negative control and *RPL15* knockdown gastric epithelial cells were used to detect Wnt signaling pathway and the expression of β-catenin/ TCF4-related target genes (cyclin D1, *Axin2* and *c-Myc*). The results showed that after knocking down *RPL15*, the expression of β-catenin and TCF4 was significantly downregulated, and the expression of SFRP1 was upregulated in *H. pylori*-infected cells (Fig. 7E). Cyclin D1, *Axin2* and *c-Myc* were downregulated in *H. pylori*-infected cells (Additional file 1: Figure S3E). *H. pylori*-infected negative control cells showed β-catenin nuclear translocation, while in the knockdown group this was not observed (Additional file 1: Figure S 4D). CFSE, colony-forming, CCK8, and EdU experiments showed that cell proliferation was weakened after *RPL15* knockdown (Fig. 7F-I). Transwell and wound healing assays showed that migration ability was weakened after *RPL15* knockdown (Fig. 7J-K).

The experimental results confirmed that under *H. pylori* infection, GGT can decrease α-KG levels and increase histone methylation, thereby leading to RPL15-related activation of the Wnt signaling pathway. RPL15 is therefore an important intermediate molecule involved in the pathogenesis of gastric cancer caused by *H. pylori* infection.

Discussion

In the current study, the gastric tissues of *H. pylori*-infected 18-month-old mice were subjected to Ki-67 immunohistochemical staining, and the *H. pylori* group had the strongest proliferative ability compared to the *H. pylori* knockout and α-KG groups. *H. pylori* supernatant-infected cells showed significantly enhanced cell proliferation and migration abilities, while *GGT* knockout of *H. pylori* and α-KG supplementation attenuated and reversed the effect, respectively. In addition, the secretion of GGT in *H. pylori* reduced the content of glutamine and α-KG, up-regulated histone H3K9me3 and H3K27me3, and activated the Wnt-related signaling pathway. Moreover, significant relative upregulation of the ribosomal protein RPL15 was detected in the gastric tissues of *H. pylori*-gavaged mice. α-KG supplementation and methylation inhibitor decreased the expression of RPL15, while *RPL15* knockdown inhibited the Wnt signaling pathway. The results confirmed that the knockdown of *RPL15* decreased cell proliferation and migration, suggesting that ribosomal proteins may be intermediate molecules in the GGT-mediated Wnt signaling pathway. Therefore, our study suggests that GGT secreted by *H. pylori* affects the energy metabolism of gastric epithelial cells, and that histone methylation status is involved in gastric carcinogenesis.

H. pylori infection can damage the gastric epithelium and is a primary risk factor for gastric cancer [25–28]. GGT damages gastric epithelial cells by producing reactive oxygen species, inducing apoptosis and cell cycle arrest, and promoting inflammatory and other pathways, making the gastric tissue more susceptible to carcinogenesis [4]. Gastric tissues were collected from *H. pylori* infected mice after gavage with *H. pylori* or *GGT* knockout *H. pylori*-infected mice for 18 months. The 16sRNA results suggested continuous *H. pylori* colonization during the mouse model establishment. Dysplasia

(See figure on next page.)

Fig. 5 Secretion of gamma-glutamyl transferase by *H. pylori* promotes the expression of RPL15. Gastric tissues were collected from *H. pylori*-infected mice and gamma-glutamyl transferase knockout *H. pylori*-infected mice for proteomic analysis ($n = 3$ per group). **A** Gene ontology analysis of tissue data of Hp and Hp-KS-1 mice. **B** Volcano plot analysis of tissue data from Hp and Hp-KS-1 mice. **C** Relative mRNA expression of RPL15 in cells and tissues of the Hp and Hp-KS-1 groups was determined by RT-qPCR ($n = 5$ in each group). **D** Representative images of RPL15 expression in cells and tissues of Hp and Hp-KS-1 groups detected by Western blot assay and the statistical analysis. Data are expressed as mean ± standard deviation. * $p < 0.05$, * *$p < 0.01$, * * * $p < 0.001$, * * * *$p < 0.0001$. Abbreviations: Hp: *H. pylori* intervention group; Hp-KS-1: gamma-glutamyl transferase knockout *H. pylori* intervention group

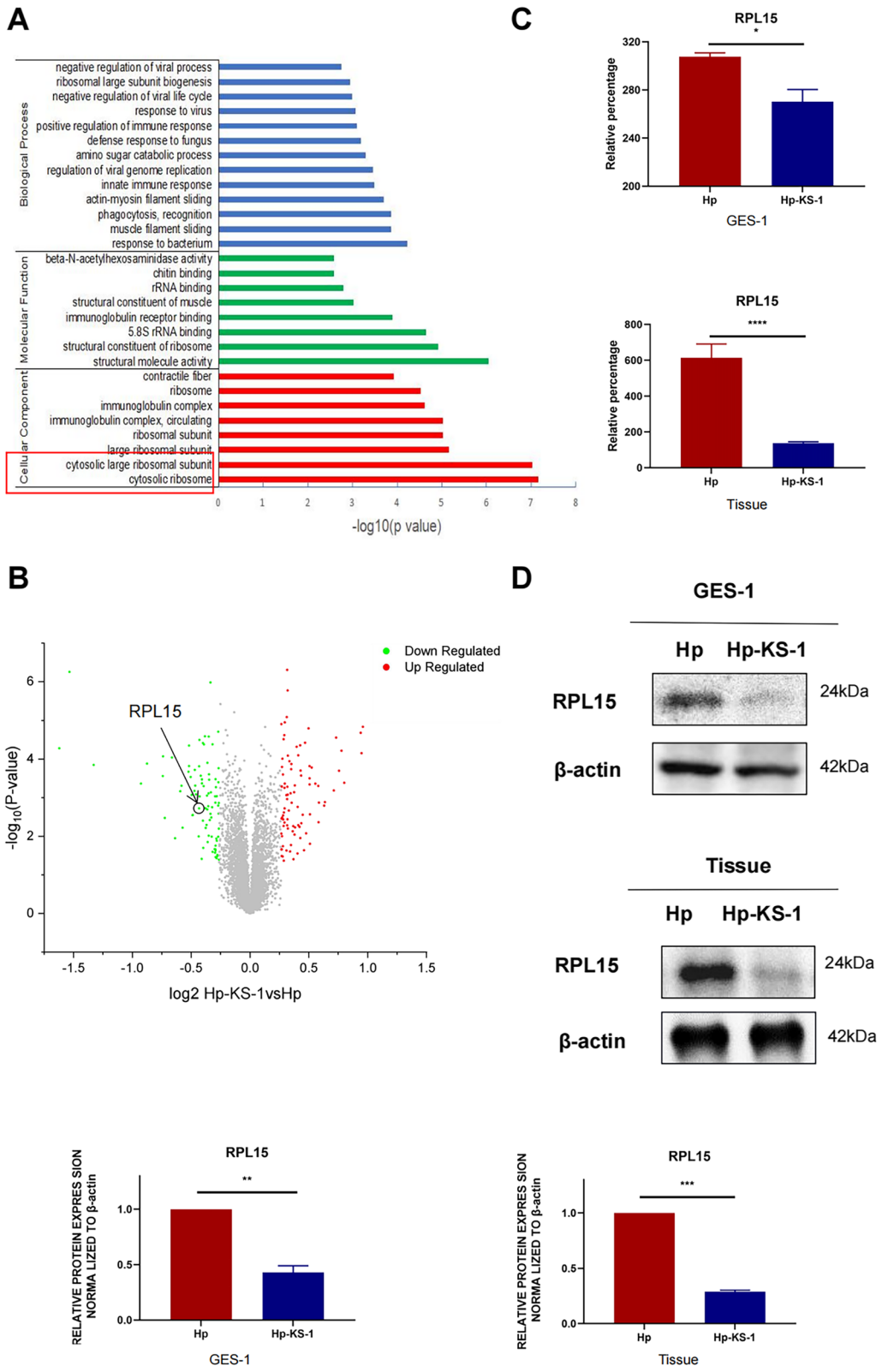

Fig. 5 (See legend on previous page.)

and developmental abnormalities were observed in *H. pylori*-infected mice, whereas *GGT* knockout *H. pylori*-infected mice exhibited reduced pathological conditions. The Ki-67 immunohistochemical results also showed vigorous cell proliferation in the *H. pylori* infection group. In vitro experiments confirmed that *H. pylori* infection enhances the proliferation and migration of gastric epithelial cells. These results suggest that GGT is an important pathogenic factor in gastric cancer; however, the specific mechanism requires further study.

GLN is an important amino acid to maintain a healthy gastrointestinal environment. GGT can consume GLN and reduce the its content in the stomach, thereby disrupting the balance and presenting abnormal pathophysiological characteristics [6, 29]. GLN is decomposed into glutamate by glutaminase, which is decomposed into α-KG by glutamate dehydrogenase to participate in the tricarboxylic acid cycle [7, 30], affecting the occurrence of related diseases. For example, α-KG supplementation significantly reduced hepatic gluconeogenesis and ameliorated hyperglycemia [31]. In in vitro hypoxic conditions, α-KG can induce the degradation of HIF-1α in Lewis lung carcinoma, which can inhibit angiogenesis in mouse tumor models and exert an antitumor effect [32]. α-KG supplementation can reduce the level of systemic inflammatory cytokines, prolonging the lifespan and reducing the morbidity of aging mice [33]. In our study, GLN and α-KG levels decreased in gastric epithelial cells treated with *H. pylori*. The proliferation and migration of gastric epithelial cells were also decreased in α-KG supplemented group. This was confirmed by tumor formation experiments in nude mice. These studies confirm that GGT secreted by *H. pylori* affects the energy metabolism of gastric epithelial cells and their biological characteristics. However, its influence on biological characteristics requires further exploration.

α-KG is a substrate of dioxygenase and plays an important role in histone and nucleic acid demethylation [34]. Previous studies have found that H3K9me3 and H3K27me3 are upregulated, and H3K9me1 and H3K27me1 are downregulated in MSCs infected with *H. pylori* [5], and supplementation of DM-αKG can reverse the increase of related trimethylation [8]. α-KG reduces the accumulation of H3K9me3 and H3K27me3 and improves age-related osteoporosis [35]. α-KG can inhibit the differentiation of brown adipocytes by inhibiting H3K4me3 and H3K36me3 [36]. Our Western blot results also showed that *H. pylori* infection significantly upregulated H3K9me3 and H3K27me3, and knockout of GGT attenuated these changes, while α-KG supplementation had opposite results. Histone methylation regulates developmental processes in organisms and plays a vital role in the occurrence and development of diseases [37]. Aberrant DNA methylation in gene promoter regions can lead to the inactivation of tumor suppressor and other cancer-related genes in cancer cells and is the clearest epigenetic marker of gastric cancer [38, 39]. The Wnt signaling pathway regulates body homeostasis and self-renewal of stem cells. Abnormal Wnt signaling can lead to related pathological changes [40] and promotes the occurrence and metastasis of gastric cancer [41–43]. Changes in DNA methylation can cause mutations in chromatin modifiers and abnormalities in the Wnt signaling pathway and promote the occurrence of related tumors [44]. It has been reported that supplementation with α-KG can reverse intestinal stemness and Wnt hyperactivation induced by low glutamine [19]. This experiment also confirmed that when α-KG or H3K27me3/H3K9me3 inhibitors BIX01294 and GSK126 were added in the experimental group [45], Wnt signaling pathway activation was weakened after trimethylation deprivation, the expression of β-catenin/TCF4-related target genes was reduced, and cell proliferation and migration were impaired. In conclusion, *H. pylori* secreted GGT reduced α-KG, an energy metabolite of gastric epithelial cells, and increased histone trimethylation, thereby activating the Wnt signaling pathway.

To further explore the relationship between the Wnt signaling pathway, altered energy metabolism, and histone methylation status in *H. pylori* infection, gastric tissues of *H. pylori* infected and *GGT* knockout *H. pylori*-infected mice were collected for proteomic analysis. The results showed that most differentially expressed proteins were ribosomal proteins. Volcano plot screening showed

(See figure on next page.)

Fig. 6 Gamma-glutamyl transferase secreted by *H. pylori* affects the energy metabolism and histone methylation of gastric epithelial cells and promotes the expression of RPL15. **A** RT-qPCR was used to detect the relative mRNA expression of RPL15 in cells and tissues of the control, Hp, Hp-KS-1, and Hp + α-KG groups ($n = 5$ in each group). **B**-**C** Representative images of RPL15 expression in cells and tissues of the control, Hp, Hp-KS-1, and Hp + α-KG groups were detected by Western blot assay and analyzed statistically. **D** The cells were divided into the Hp, Hp-KS-1, and Hp + α-KG groups, with BIX01294 and GSK126 inhibitor added on the basis of these conditions, respectively. Representative images of RPL15 expression in each group were detected by Western blot and analyzed statistically. Data are expressed as mean ± standard deviation. In all groups: * $p < 0.05$, * * $p < 0.01$, * * * $p < 0.001$, * * * * $p < 0.0001$. Abbreviations: BIX01294: G9a histone methyltransferase inhibitor; GSK126: EZH2 methyltransferase inhibitor; Hp: *H. pylori* intervention group; Hp + α-KG: Hp and α-KG supplementation group; Hp-KS-1: gamma-glutamyl transferase knockout *H. pylori* intervention group

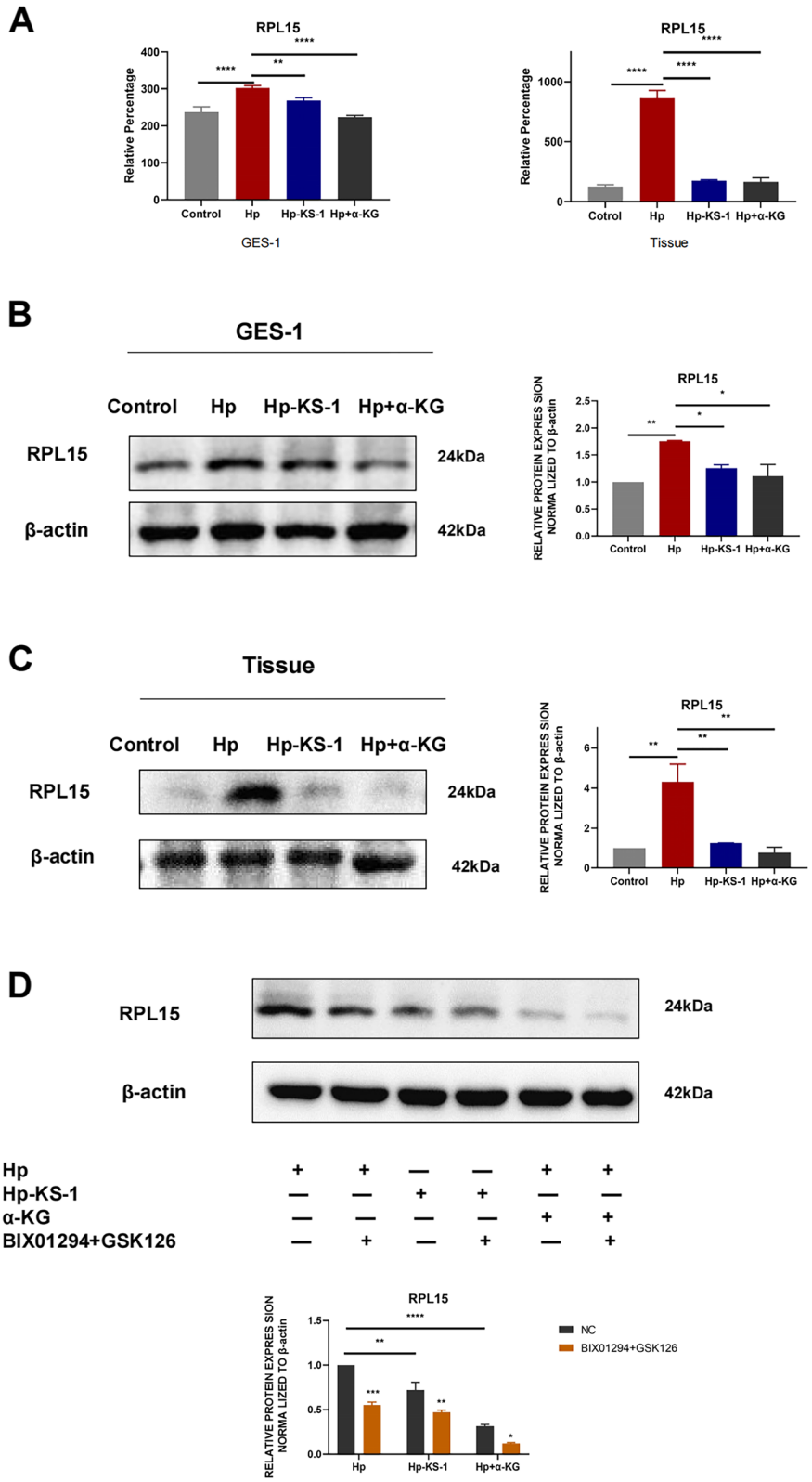

Fig. 6 (See legend on previous page.)

that the ribosomal protein RPL15 significantly decreased after *GGT* knockout. RPL15 is derived from eukaryotic ribosomal 60S subunit [46]. When RPL15 is overexpressed, the number of nucleoli and the expression of nucleolar proteins increases, and the abnormal increase in nucleolar size and number caused by dysregulation of ribosome biosynthesis is a hallmark of most spontaneous cancers [47]. Overexpression of RPL15 increases breast cancer metastasis [48]; this expression is also upregulated in esophageal cancer [49] and in gastric cancer tissues, whereas the growth of gastric cancer cells with *RPL15* knockdown is significantly restricted [22]. This was confirmed using PCR and Western blotting. Later, in-depth exploration revealed that MYC is pivotal in the regulation of ribosomal function and protein synthesis, facilitating the synthesis of proteins such as RPL15 [50–52]. The inhibition of H3K27 and H3K9 methyltransferases can inhibit H3K27me3/H3K9me3 methylation and downregulate *MYC* [53]. Under H_2O_2 treatment, ribosomal proteins are subjected to oxidative stress via the n-Myc pathway, in which the ribosomal protein RPL15 expression is significantly increased [52]. Accordingly, we hypothesized that increased histone trimethylation favors RPL15 expression. The results also show that the expression of RPL15 is increased in *H. pylori*-infected cells or tissues and decreased by α-KG supplementation. We also applied BIX01294 and GSK126 [45], which are inhibitors of H3K27me3/H3K9me3, and found that with the reduction of H3K9 and H3K27 trimethylation, the expression of RPL15 also decreased. Therefore, gamma-glutamyl transferase secreted by *H. pylori* affects energy metabolism, the histone methylation status of gastric epithelial cells, and consequently the expression of RPL15.

It has been reported that MYC and Wnt/β-catenin signaling pathways synergistically promote the occurrence of lung squamous cell carcinoma [54]. Up-regulation of n-Myc leads to overexpression of RPL15, sustained over-activation of ribosome biogenesis, and selective enhancement of β-catenin, which may be involved in tumorigenesis of offspring of oxidative damage embryos through cross-interactions with Wnt and TGF-β1 pathways [52, 55]. Therefore, we speculate that there is a relationship between RPL15 and the Wnt signaling pathway. For further confirmation, the results of immunofluorescence, Western blotting, and PCR showed that the nuclear translocation of β-catenin was detected in *H. pylori*-infected cells, while the deletion of *RPL15* led to a reversal of this translocation. After simultaneously knocking down *RPL15*, the expression of Wnt signaling pathway inhibitor proteins was increased and the expression of related target genes was downregulated, indicating that the Wnt signaling pathway was weakened. Finally, we comprehensively verified that GGT mediated the activation of Wnt signaling pathway by RPL15 through its effects on energy metabolism and histone methylation status in GES-1 under *H. pylori* infection. Western blot, PCR, and immunofluorescence results showed that the expression of the Wnt signaling pathway-related proteins β-catenin and TCF4, as well as the expression of β-catenin/TCF4-related target genes, was significantly increased in the *H. pylori* group, and ectopic nuclear translocation of β-catenin occurred. The expression was decreased after *GGT* knockout and reversed after α-KG supplementation. Knockdown of RPL15 decreased the protein expressions of β-catenin, TCF4, and related target genes, and did not cause β-catenin translocation into the nucleus. Knockdown of RPL15 reduced cell proliferation and migration in vitro.

On this basis, we conclude that GGT secreted by *H. pylori* can promote the expression of Wnt signaling pathway related proteins through RPL15 by reducing the expression of α-KG and up-regulating the trimethylation of H3K9 and H3K27, thereby leading to the occurrence of gastric cancer. Supplementation of glutamine, α-KG and knockdown of *RPL15* could reverse the condition.

(See figure on next page.)

Fig. 7 Gamma-glutamyl transferase secreted by *H. pylori* affects energy metabolism and histone methylation of gastric epithelial cells, activates Wnt signaling pathway through RPL15, and increases the proliferation and migration of gastric epithelial cells. **A** Representative immunofluorescence images of cells in the negative control of GES-1 only, negative control with *H. pylori* infection (HP + GES-1 + NC siRNA), and RPL15 knockdown group of *H. pylori* infection (HP + GES-1 + RPL15 siRNA). **B**-**C** Representative images of β-catenin, TCF4, and SFRP1 expression in gastric epithelial cells and gastric tissues of the control, Hp, Hp-KS-1, and Hp + α-KG groups were detected by Western blotting and statistically analyzed. **D** The cells were divided into Hp, Hp-KS-1, and Hp + α-KG groups, with BIX01294 and GSK126 inhibitor added on separately to each of these groups. Representative images of β-catenin, TCF4, and SFRP1 expression in each group were detected by Western blotting and analyzed statistically. **E** Negative control cells and RPL15 knockdown cells were divided into six groups with *H. pylori* supernatant, *H. pylori* supernatant with gamma-glutamyl transferase knockout, and *H. pylori* supernatant with α-KG. Representative images of β-catenin, TCF4, RPL15 and SFRP1 expression in the six groups were detected by Western blotting and analyzed statistically. **F**-**K** CFSE, Colony-forming experiment, CCK8, EdU cell proliferation assay, transwell experiment, and wound healing results of negative control and RPL15 knockdown cells and their respective intervention groups, and the corresponding statistical analysis. Data are expressed as mean ± standard deviation. * $p < 0.05$, * *$p < 0.01$, * * * $p < 0.001$, * * * *$p < 0.0001$. Abbreviations: CCK8: Cell Counting Kit-8; CFSE: Fluorescent label carboxyfluorescein diacetate succinimidyl ester; Hp: *H. pylori* intervention group; Hp-KS-1: gamma-glutamyl transferase knockout *H. pylori* intervention group; Hp + α-KG: Hp and α-KG supplementation group

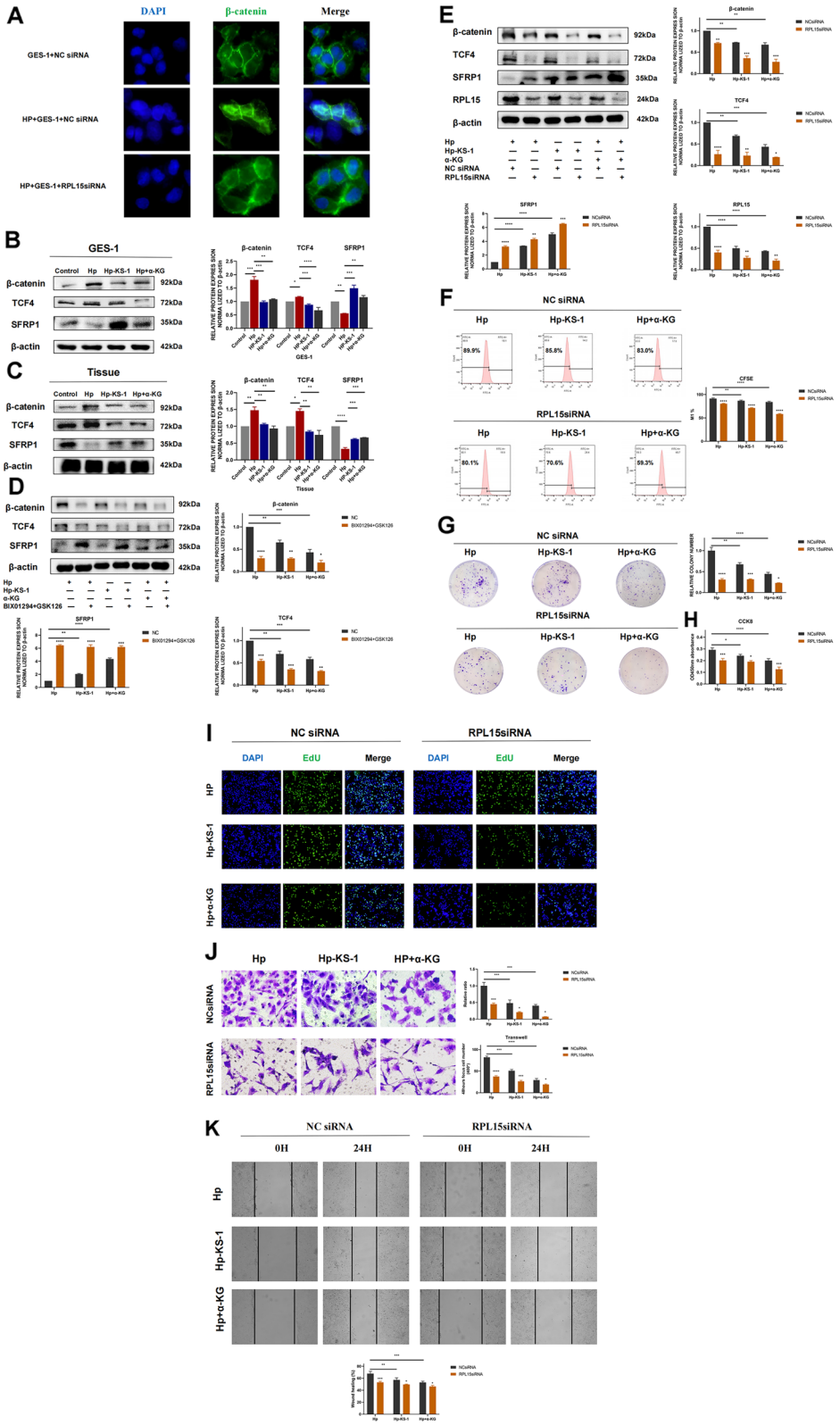

Fig. 7 (See legend on previous page.)

This may be a promising approach for the prevention and treatment of gastric carcinogenesis.

GGT has a profound effect on gastric epithelial cells, and it should be extremely interesting to study the specific mechanisms. According to a previous report, highly purified *Escherichia coli* secreted GGT is an ideal model for the study of enzyme reaction mechanisms [56]. The study of GGT protein processing in vitro is therefore promising to determine changes that caused gastric cancer. Further studies on the expression of GGT in gastric epithelial cells and how it affects cell metabolism will also help us understand the pathogenesis of gastric diseases caused by *H. pylori*, making these very interesting areas to explore; they will also be the focus of our future research. In conclusion, our experimental study provides new insights into the mechanism of *H. pylori* secreted GGT in the development of gastric cancer.

Abbreviations

GGT	Gamma-glutamyl transferase
H. pylori	*Helicobacter pylori*
MSC	Mesenchymal stem cells
α-KG	Alpha-ketoglutarate
TCA	Tricarboxylic acid
OD	Optical density
PCR	Polymerase chain reaction
PBS	Phosphate buffered saline
SFRP1	Secreted frizzled related protein 1
siRNA	Small interfering RNA
GLN	Glutamine

Supplementary Information

The online version contains supplementary material available at https://doi.org/10.1186/s12964-024-01780-x.

Additional file 1: Figure S1. NCBI alignment of *H. pylori* 16SRNA in mice gastric tissues. *H. pylori* in gastric tissues of mice in Hp group, Hp-KS-1 group and Hp+α-KG group were collected and cultured. The bacterial DNA was extracted for 16sRNA, and the sequencing results were compared with the NCBI database. Figure S2. RPL15 activates the Wnt signaling pathway. Representative images of β-catenin, TCF4, and SFRP1 expression in negative control with GES-1 only, negative control with *H. pylori* infection, and RPL15 knockdown group of *H. pylori* infection-were detected by Western blot assay and analyzed statistically. Data are expressed as mean ± standard deviation. * *p* < 0.01, * * * *p* < 0.001, * * * *p* < 0.0001. Figure S3. Expression of β-catenin/TCF4 related target genes cyclin D1, Axin 2, and c-Myc in different groups.(A) RT-qPCR was used to detect the relative expression of cyclin D1, Axin 2, and c-Myc mRNA in the gastric epithelial cell negative control, *H. pylori* infection (HP+GES-1+NC siRNA), and *H. pylori* infection RPL15 knockdown (HP+GES-1+RPL15 siRNA) groups. (B-C) RT-qPCR was used to detect the relative expression of cyclin D1, Axin 2, and c-Myc mRNA in gastric epithelial cells and gastric tissues of the control, Hp, Hp-KS-1, and Hp+α-KG groups. (D) RT-qPCR was used to detect the relative expression of cyclin D1, Axin 2, and c-Myc mRNA in the Hp, Hp-KS-1, Hp+α-KG, and corresponding inhibitor groups. (E) RT-qPCR was used to detect the relative expression of cyclin D1, Axin 2, and c-Myc mRNA in the Hp, Hp-KS-1, Hp+α-KG negative control, and corresponding RPL15 knockdown groups. Data are expressed as mean ± standard deviation. * *p*< 0.05, * *p* < 0.01, * * * *p* < 0.001, * * * *p* < 0.0001. Abbreviations: Hp: *H. pylori* intervention group; Hp-KS-1: gamma-glutamyl transferase knockout *H. pylori* intervention group; Hp+α-KG: Hp and α-KG supplementation group. Figure S4. Immunofluorescence localization of β-catenin in different groups.Representative immunofluorescence images of gastric epithelial cells and gastric tissue in the control, Hp, Hp-KS-1, and Hp+α-KG group.Representative cell immunofluorescence images of the Hp, Hp-KS-1, Hp+α-KG group, and corresponding inhibitor groups .Representative immunofluorescence images of cells in the Hp, Hp-KS-1, Hp+α-KG negative control, and corresponding RPL15 knockdown groups.

Additional file 2.

Additional file 3.

Acknowledgements
The authors thank all those who contributed to this article, including Figdraw.

Authors' contributions
XJ and WJW designed the study, performed the experiments, and wrote the manuscript; ZYW and ZW assisted in the experimental design ; HYS, LJM, SYP and MKF helped to analyze some data ; RL designed and supervised the experiments. All authors read and approved the final manuscript.

Funding
This work was supported by the National Key Research and Development Program of China (Nos.2023YFC2307001),National Natural Science Foundation of China (Nos. 82170571,81974068,81572428,81900580and82270586),Natural Science Foundation of Hubei Province(Nos. 2022CFA009).

Availability of data and materials
The datasets supporting the conclusions of this article are included within the article and its additional files.

Data availability
No datasets were generated or analysed during the current study.

Declarations

Ethics approval and consent to participate
All experimental procedures were performed in accordance with institutional guideline and were approved by the Animal Ethics Committee of the Tongji Medical College, Huazhong University of Science and Technology and the Medical Ethics Committee of Wuhan Union Hospital. (S-028.19–12-12).

Consent for publication
All authors agree to publication.

Competing interests
The authors declare no competing interests.

Author details
[1]Department of Gastroenterology, Union Hospital, Tongji Medical College, Huazhong University of Science and Technology, Wuhan 430022, China.

Received: 21 January 2024 Accepted: 6 August 2024
Published online: 15 August 2024

References

1. Bray F, Ferlay J, Soerjomataram I, Siegel RL, Torre LA, Jemal A. Global cancer statistics 2018: GLOBOCAN estimates of incidence and mortality worldwide for 36 cancers in 185 countries. CA Cancer J Clin. 2018;68:394–424.
2. Wang F, Meng W, Wang B, Qiao L. Helicobacter pylori-induced gastric inflammation and gastric cancer. Cancer Lett. 2014;345:196–202.
3. Gong M, Ling SS, Lui SY, Yeoh KG, Ho B. Helicobacter pylori gamma-glutamyl transpeptidase is a pathogenic factor in the development of peptic ulcer disease. Gastroenterology. 2010;139:564–73.
4. Ling SS, Yeoh KG, Ho B. Helicobacter pylori γ-glutamyl transpeptidase: a formidable virulence factor. World J Gastroenterol. 2013;19:8203–10.
5. Wang Z, Wang W, Shi H, Meng L, Jiang X, Pang S, et al. Gamma-glutamyltransferase of Helicobacter pylori alters the proliferation, migration, and

pluripotency of mesenchymal stem cells by affecting metabolism and methylation status. J Microbiol. 2022;60:627–39.
6. Shibayama K, Wachino J, Arakawa Y, Saidijam M, Rutherford NG, Henderson PJ. Metabolism of glutamine and glutathione via gamma-glutamyltranspeptidase and glutamate transport in Helicobacter pylori: possible significance in the pathophysiology of the organism. Mol Microbiol. 2007;64:396–406.
7. Baksh SC, Finley LWS. Metabolic Coordination of Cell Fate by α-Ketoglutarate-Dependent Dioxygenases. Trends Cell Biol. 2021;31:24–36.
8. Carey BW, Finley LW, Cross JR, Allis CD, Thompson CB. Intracellular α-ketoglutarate maintains the pluripotency of embryonic stem cells. Nature. 2015;518:413–6.
9. Amagase K, Nakamura E, Endo T, Hayashi S, Hasumura M, Uneyama H, et al. New frontiers in gut nutrient sensor research: prophylactic effect of glutamine against Helicobacter pylori-induced gastric diseases in Mongolian gerbils. J Pharmacol Sci. 2010;112:25–32.
10. Martinez S, Hausinger RP. Catalytic Mechanisms of Fe (II)- and 2-Oxoglutarate-dependent Oxygenases. J Biol Chem. 2015;290:20702–11.
11. Zdzisińska B, Żurek A, Kandefer-Szerszeń M. Alpha-Ketoglutarate as a Molecule with Pleiotropic Activity: Well-Known and Novel Possibilities of Therapeutic Use. Arch Immunol Ther Exp (Warsz). 2017;65:21–36.
12. Chung C, Sweha SR, Pratt D, Tamrazi B, Panwalkar P, Banda A, et al. Integrated Metabolic and Epigenomic Reprograming by H3K27M Mutations in Diffuse Intrinsic Pontine Gliomas. Cancer Cell. 2020;38(3):334–9.e9.
13. Baksh SC, Todorova PK, Gur-Cohen S, Hurwitz B, Ge Y, Novak JSS, et al. Extracellular serine controls epidermal stem cell fate and tumour initiation. Nat Cell Biol. 2020;22:779–90.
14. Yamada H, Takeshima H, Fujiki R, Yamashita S, Sekine S, Ando T, et al. ARID1A loss-of-function induces CpG island methylator phenotype. Cancer Lett. 2022;532: 215587.
15. Logan CY, Nusse R. The Wnt signaling pathway in development and disease. Annu Rev Cell Dev Biol. 2004;20:781–810.
16. Clevers H. Wnt/beta-catenin signaling in development and disease. Cell. 2006;127:469–80.
17. Yousefi B, Mohammadlou M, Abdollahi M, Salek Farrokhi A, Karbalaei M, Keikha M, et al. Epigenetic changes in gastric cancer induction by Helicobacter pylori. J Cell Physiol. 2019;234:21770–84.
18. Yong X, Tang B, Xiao YF, Xie R, Qin Y, Luo G, et al. Helicobacter pylori upregulates Nanog and Oct4 via Wnt/β-catenin signaling pathway to promote cancer stem cell-like properties in human gastric cancer. Cancer Lett. 2016;374:292–303.
19. Tran TQ, Hanse EA, Habowski AN, Li H, Ishak Gabra MB, Yang Y, et al. α-Ketoglutarate attenuates Wnt signaling and drives differentiation in colorectal cancer. Nat Cancer. 2020;1:345–58.
20. Pate KT, Stringari C, Sprowl-Tanio S, Wang K, TeSlaa T, Hoverter NP, et al. Wnt signaling directs a metabolic program of glycolysis and angiogenesis in colon cancer. EMBO J. 2014;33:1454–73.
21. Meng L, Shi H, Wang Z, Fan M, Pang S, Lin R. The Gamma-glutamyltransferase gene of Helicobacter pylori can promote gastric carcinogenesis by activating Wnt signal pathway through up-regulating TET1. Life Sci. 2021;267: 118921.
22. Wang H, Zhao LN, Li KZ, Ling R, Li XJ, Wang L. Overexpression of ribosomal protein L15 is associated with cell proliferation in gastric cancer. BMC Cancer. 2006;6:91.
23. Cao L, Zhu S, Lu H, Soutto M, Bhat N, Chen Z, et al. Helicobacter pylori-induced RASAL2 Through Activation of Nuclear Factor-κB Promotes Gastric Tumorigenesis via β-catenin Signaling Axis. Gastroenterology. 2022;162:1716–31.e17.
24. Lin S, Yan Z, Tang Q, Zhang S. Ubiquitin-associated protein 2 like (UBAP2L) enhances growth and metastasis of gastric cancer cells. Bioengineered. 2021;12:10232–45.
25. Amieva M, Peek RM Jr. Pathobiology of Helicobacter pylori-Induced Gastric Cancer. Gastroenterology. 2016;150:64–78.
26. Lee YC, Chiang TH, Chou CK, Tu YK, Liao WC, Wu MS, Graham DY. Association Between Helicobacter pylori Eradication and Gastric Cancer Incidence: A Systematic Review and Meta-analysis. Gastroenterology. 2016;150:1113–24.e5.
27. Stewart OA, Wu F, Chen Y. The role of gastric microbiota in gastric cancer. Gut Microbes. 2020;11:1220–30.
28. Mentis AA, Boziki M, Grigoriadis N, Papavassiliou AG. Helicobacter pylori infection and gastric cancer biology: tempering a double-edged sword. Cell Mol Life Sci. 2019;76:2477–86.
29. De Bruyne E, Ducatelle R, Foss D, Sanchez M, Joosten M, Zhang G, et al. Oral glutathione supplementation drastically reduces Helicobacter-induced gastric pathologies. Sci Rep. 2016;6:20169.
30. Corbet C, Feron O. Metabolic and mind shifts: from glucose to glutamine and acetate addictions in cancer. Curr Opin Clin Nutr Metab Care. 2015;18:346–53.
31. Yuan Y, Zhu C, Wang Y, Sun J, Feng J, Ma Z, et al. α-Ketoglutaric acid ameliorates hyperglycemia in diabetes by inhibiting hepatic gluconeogenesis via serpina1e signaling. Sci Adv. 2022;8:eabn2879.
32. Matsumoto K, Obara N, Ema M, Horie M, Naka A, Takahashi S, et al. Antitumor effects of 2-oxoglutarate through inhibition of angiogenesis in a murine tumor model. Cancer Sci. 2009;100:1639–47.
33. Shahmirzadi AA, Edgar D, Liao CY, Hsu YM, Lucanic M, Shahmirzadi AA, et al. Alpha-ketoglutarate, an endogenous metabolite, extends lifespan and compresses morbidity in aging mice. Cell Metab. 2020;32:447–56.e6.
34. Loenarz C, Schofield CJ. Expanding chemical biology of 2-oxoglutarate oxygenases. Nat Chem Biol. 2008;4:152–6.
35. Wang Y, Deng P, Liu Y, Wu Y, Chen Y, Guo Y, et al. Alpha-ketoglutarate ameliorates age-related osteoporosis via regulating histone methylations. Nat Commun. 2020;11:5596.
36. Kang HS, Lee JH, Oh KJ, Lee EW, Han BS, Park KY, et al. IDH1-dependent α-KG regulates brown fat differentiation and function by modulating histone methylation. Metabolism. 2020;105: 154173.
37. Jambhekar A, Dhall A, Shi Y. Roles and regulation of histone methylation in animal development. Nat Rev Mol Cell Biol. 2019;20:625–41.
38. Qu Y, Dang S, Hou P. Gene methylation in gastric cancer. Clin Chim Acta. 2013;424:53–65.
39. Chen ZH, Yan SM, Chen XX, Zhang Q, Liu SX, Liu Y, et al. The genomic architecture of EBV and infected gastric tissue from precursor lesions to carcinoma. Genome Med. 2021;13:146.
40. Clevers H, Nusse R. Wnt/β-catenin signaling and disease. Cell. 2012;149:1192–205.
41. Dong M, Gong LP, Chen JN, Zhang XF, Zhang YW, Hui DY, et al. EBV-miR-BART10-3p and EBV-miR-BART22 promote metastasis of EBV-associated gastric carcinoma by activating the canonical Wnt signaling pathway. Cell Oncol (Dordr). 2020;43:901–13.
42. Katoh M. Multi-layered prevention and treatment of chronic inflammation, organ fibrosis and cancer associated with canonical WNT/β-catenin signaling activation (Review). Int J Mol Med. 2018;42:713–25.
43. Cancer Genome Atlas Research Network. Comprehensive molecular characterization of gastric adenocarcinoma. Nature. 2014;513:202–9.
44. Saghafinia S, Mina M, Riggi N, Hanahan D, Ciriello G. Pan-Cancer Landscape of Aberrant DNA Methylation across Human Tumors. Cell Rep. 2018;25:1066–80.e8.
45. Sherzai M, Valle A, Perry N, Kalef-Ezra E, Al-Mahdawi S, Pook M, et al. HMTase inhibitors as a potential epigenetic-based therapeutic approach for friedreich's ataxia. Front Genet. 2020;11:584.
46. Baßler J, Hurt E. Eukaryotic ribosome assembly. Annu Rev Biochem. 2019;88:281–306.
47. Hald ØH, Olsen L, Gallo-Oller G, Elfman LHM, Løkke C, Kogner P, et al. Inhibitors of ribosome biogenesis repress the growth of MYCN-amplified neuroblastoma. Oncogene. 2019;38:2800–13.
48. Ebright RY, Lee S, Wittner BS, Niederhoffer KL, Nicholson BT, Bardia A, et al. Deregulation of ribosomal protein expression and translation promotes breast cancer metastasis. Science. 2020;367:1468–73.
49. Wang Q, Yang C, Zhou J, Wang X, Wu M, Liu Z. Cloning and characterization of full-length human ribosomal protein L15 cDNA which was overexpressed in esophageal cancer. Gene. 2001;263:205–9.
50. Boon K, Caron HN, van Asperen R, Valentijn L, Hermus MC, van Sluis P, et al. N-myc enhances the expression of a large set of genes functioning in ribosome biogenesis and protein synthesis. EMBO J. 2001;20:1383–93.
51. Destefanis F, Manara V, Bellosta P. Myc as a Regulator of Ribosome Biogenesis and Cell Competition: A Link to Cancer. Int J Mol Sci. 2020;21:4037.
52. Huang Y, Li Z, Lin E, He P, Ru G. Oxidative damage-induced hyperactive ribosome biogenesis participates in tumorigenesis of offspring by

cross-interacting with the Wnt and TGF-β1 pathways in IVF embryos. Exp Mol Med. 2021;53:1792–806.
53. Ishiguro K, Kitajima H, Niinuma T, Maruyama R, Nishiyama N, Ohtani H, et al. Dual EZH2 and G9a inhibition suppresses multiple myeloma cell proliferation by regulating the interferon signal and IRF4-MYC axis. Cell Death Discov. 2021;7:7.
54. Liu W, Fu X, Li R. CNN1 regulates the DKK1/Wnt/β-catenin/c-myc signaling pathway by activating TIMP2 to inhibit the invasion, migration and EMT of lung squamous cell carcinoma cells. Exp Ther Med. 2021;22:855.
55. Davuluri G, Giusto M, Chandel R, Welch N, Alsabbagh K, Kant S. Impaired ribosomal biogenesis by noncanonical degradation of β-Catenin during hyperammonemia. Mol Cell Biol. 2019;39:e00451–e518.
56. Okada T, Suzuki H, Wada K, Kumagai H, Fukuyama K. Crystal structures of gamma-glutamyltranspeptidase from Escherichia coli, a key enzyme in glutathione metabolism, and its reaction intermediate. Proc Natl Acad Sci U S A. 2006;103:6471–6.

Publisher's Note

Springer Nature remains neutral with regard to jurisdictional claims in published maps and institutional affiliations.